

### Abstract

Particle image velocimetry (PIV) is applied for the first time to study Eckart streaming induced by a medical ultrasonic transducer operating at 0.25 and 3 Wcm<sup>-2</sup>. A temporal series of velocities in a two-dimensional plane were recorded resulting in an experimental set comprising over half a million velocity data points. These enabled average and fluctuating properties to be determined and clearly indicated the quasi-steady nature of the flow. The average large-scale velocity fluctuations along the axis caused by this quasi-steady property were calculated to be 2 and 20 mms<sup>-1</sup> for transducer settings of 0.25 and 3 Wcm<sup>-2</sup> respectively corresponding to approximately 25 % of the peak flow velocity in both cases. Furthermore averaged shear rates were calculated with peak values of 1 and 8 s<sup>-1</sup> for the low and high intensities respectively. The present investigation indicates the usefulness of PIV for such studies and serves as a prelude to investigations of streaming in biological type fluids.

## 1 Introduction

Particle image velocimetry (PIV) is a velocity measuring technique [1] which has been used extensively in fluid dynamics to study a vast range of flow problems. It has also been applied in a limited manner to the measurement of the velocity of a

sound field [2], although our concern here is with measuring the streaming velocity, not the oscillatory velocity of the ultrasound waves. Eckart streaming is a steady-state velocity generated by the attenuation of the sound wave in a viscous fluid. Here we are concerned with applying PIV to ultrasonic Eckart streaming in water as a prelude to further investigations in biological fluids. Particulate phases are inherent in these fluids and thus are ideal for PIV analyses.

PIV enables two-dimensional (and in some applications three-dimensional) instantaneous velocity maps to be obtained. The results allow an immediate visual assesment of the spatial structure of the flow and furthermore enable kinematic quantities such as instantaneous shear and vorticity to be easily derived [3]. Recently, streaming has been investigated using point measuring techniques by a number of authors, see for example [4, 5, 6, 7]. Full field velocity measurements were obtained using PIV [8] for Rayleigh streaming in air at a frequencies of 2460 and 1910 Hz, however this is the first investigation of Eckart streaming using PIV. A description is now given of the experimental apparatus and methods used.

## 2 Experimental apparatus

The illumination system consisted of a 300 mW continuous wave Nd-Yag laser, collimating and beam steering optics, an octagonal-rotating mirror and a parabolic mirror arranged as shown in Figure 1. Light from the laser (with a wavelength  $\lambda = 532$  nm) was directed onto the octagonal mirror via the collimating and steering optics. Rotation of the octagonal mirror caused the beam to be swept repeatedly in an arc onto the parabolic mirror which in turn directed the laser beam vertically through the bottom of the glass tank. A mechanical shutter placed between the

light source and rotating mirror enabled the pseudo-light sheet to be turned on and off. The rotational speed of the octagonal mirror could be varied in the range 50 - 250 rps corresponding to sweep intervals of 2.5 to 0.5 ms. A light sensitive diode placed in the path of the beam generated a signal for every sweep of the beam indicating an accuracy of greater than  $\pm 0.05$  ms per sweep.

The particulate phase of the solution consisted of polymer particles with a diameter of  $20 \pm 2 \mu\text{m}$  and relative density of 1.03 which were mixed in with the liquid. It has been shown that these particles follow the fluid very accurately [9]. These acted as scattering sites for the laser light. The side scattered light from the particles was focussed onto a digital PCO camera using a 55mm Micro-Nikkor lens (with  $f^\# = 2.8$ ). The camera exposure and particle illumination were synchronised by computer software which controlled the camera recording and exposure time. Furthermore the software controlled timing electronics connected to the mechanical chopper. The PCO camera was used in double image capture mode (the camera is capable of operating in one of several modes) which enabled two separate images to be recorded with a variable separation time. The minimum separation time used was 10 ms corresponding to the maximum output intensity of  $3 \text{ Wcm}^{-2}$ . Vector fields were produced for each image pair by interrogating small sub-regions of the images and performing a correlation algorithm to determine the average displacement between the images of the particles. An interrogation region of  $32 \times 32$  pixels and a  $16 \times 16$  grid spacing were used. Due to random effects, such as the intermittent lack of seeding in areas of an image, spurious vectors (outlier vectors) are produced. A local median filter is used to validate and interpolate the data.

A Therasonic 1030 medical ultrasonic transducer was placed in a glass tank

(600 mm long  $\times$  300 mm wide  $\times$  400 mm deep) as shown in Figure 1. The transducer was operated in continuous mode, with output intensities of 0.25 and 3  $\text{Wcm}^{-2}$ . The tank was filled with tap water via a 5  $\mu\text{m}$  filter to a depth of 300 mm (54 litres) and a National Physics Laboratory (NPL) absorber was placed at the end of the tank to avoid reflections. An area, approximately 110 mm  $\times$  100 mm immediately in front of the probe comprised the measurement region. All electronic equipment were allowed to run for 1 hour to ensure stable operating conditions. For each intensity setting the streaming was allowed to develop for ten minutes to remove transient behaviour. After this a series of 50 image pairs were captured with a ten second interval between each successive image pair. For each intensity setting the temperature of the liquid was monitored however no temperature change was observed within a  $\pm 1^\circ\text{C}$  tolerance.

### 3 Results and Discussion

Figure 2 shows an instantaneous<sup>1</sup> velocity map with the probe set to 0.25  $\text{Wcm}^{-2}$ . This map gives an immediate rendering of the spatial flow pattern, a rendering not obtained easily using point measurement techniques such as Laser Doppler Anemometry (LDA), ultrasonic Doppler (UD) or hot-wire anemometry. The axial velocity,  $v_x$ , generally increases with increasing distance from the tip of the probe in the axial direction while decreasing away from the centre of the beam in the radial direction. Velocity fluctuations superimposed on these general trends are observed

---

<sup>1</sup>The time-interval between two successive raw data images, which constitute a single vector map, is approximately 100 ms for the probe output of 0.25  $\text{Wcm}^{-2}$  and 10 ms for the probe output of 3  $\text{Wcm}^{-2}$ . This time scale is small compared with the time over which appreciable fluctuations are noted in the second order streaming and hence the word instantaneous is used. However it should be noted that these time scales represent an averaging over several thousands of sonic cycles

and are consistent with previous experimental investigation using LDA or UD [5, 7]. The Reynolds number of the flow (given by  $Re = UL/\nu$ , where  $U$  is the peak fluid velocity and  $L$  is the width of the fluid jet), indicates the relative importance of hydrodynamical nonlinearities [10] and hence the stability of the flow. For this study  $Re$  has values of approximately 180 and 1280 for the  $0.25 \text{ Wcm}^{-2}$  and  $3.0 \text{ Wcm}^{-2}$  intensity settings respectively. Evidently, the streaming sets up large scale circulations in the enclosed tank. As the Reynolds number increases these circulations become increasingly unstable, interacting with the induced jet of streaming, producing a quasi-steady flow. This is seen in Figure 3 where a large anti-clockwise rotating circulation impinges on the jet. A time series of vector maps is obtained which allows averaged quantities to be calculated. Figure 4 shows that the averaging process reduces the component of the flow associated with the large scale fluctuation, although the field is not fully symmetric. From the above discussion on Reynolds number turbulent fluctuations are to be expected, superimposed on the large scale fluctuations. If we subtract the instantaneous maps from the temporally averaged mean, then the large scale velocity fluctuations of the large scale jet-circulation interaction will dominate the turbulent fluctuations. This is shown in Figure 5 where two different methods of averaging have been used. The first method of averaging, referred to as a fixed average was obtained using a standard temporal average. A second average, referred to as a central average was obtained by centering the jet so that the maximum value of  $v_x$ , for each  $x$ -position, occurs at  $y = 0$  and then a standard temporal average was applied to the shifted data. Both these averages are shown in Figure 5 as well as the instantaneous peak velocity from one of the data sets. The difference between the instantaneous velocity and the fixed average gives

a measure of the instabilities due to the quasi-steady nature of the flow, while the difference between the instantaneous velocity and the central average gives a measure of fluctuations due other sources, for example turbulence. Clearly the former is significantly larger than the latter.

PIV enables important properties of the flow which depend on velocity gradients to be easily derived from the measurements. These quantities are not readily available from point measurement techniques such as hot-wire, LDA or UD and are important in assessing for example the stress on cell structures caused by streaming [4]. Figure 6 shows the instantaneous rate-of-shear strain,  $\gamma = \partial v_x / \partial y + \partial v_y / \partial x$  for a probe intensity of  $0.25 \text{ Wcm}^{-2}$ . It can be seen that the region in which the maximum shear is generated is close to the boundary of the streaming jet at approximately  $y = \pm 10 \text{ mm}$ . Averaged shears calculated for intensities of  $0.25$  and  $3 \text{ Wcm}^{-2}$  were approximately  $1$  and  $8 \text{ s}^{-1}$ .

## 4 Conclusions and Future Work

PIV has been successfully applied to measure the acoustic streaming velocity field produced by an ultrasonic probe in water. The two-dimensional velocity measurements enabled the streaming to be observed in detail highlighting the quasi-steady nature of the flow. Large scale velocity fluctuations associated with this were quantified as well as rates-of-shear strain. We note that the measurements are taken in the nearfield of the probe. The pressure field is, therefore, not that of a plane propagating wave, but a complex interference pattern [11]. Further work is required to quantify the relative importance of circulations, turbulence and the nearfield pressure field on the instantaneous streaming velocity.

# References

- [1] R. J. Adrian. *Annual Review of Fluid Mechanics*, 23:261–304, 1991.
- [2] M. Campbell, J. A. Cosgrove, C. A. Greated, S. Jack, and D. Rockliff. *Optics & Laser Technology*, 32:629–639, 2000.
- [3] X. Ni, J. A. Cosgrove, A. D. Arnott, C. A. Greated, and R. H. Cumming. *Chemical Engineering Science*, 55:3195–3208, 2000.
- [4] H.C. Starritt, Duck F. A., and V. F. Humphrey. *Ultrasound in Medicine and Biology*, 14(4):363–373, 1989.
- [5] G. Zauhar, H.C. Starritt, and Duck F. A. *The British Journal of Radiology*, 71:297–302, 1998.
- [6] T. G. Hertz, S. O. Dymling, K. Lindström, and H. W. Persson. *Rev. Sci. Instrum.*, 62:457–462, 1991.
- [7] H. Mitome. *Electronics and Communications in Japan, Part 3*, 81:1–8, 1998.
- [8] J. P. Sharpe, C. A. Greated, C. Gray, and D. M. Campbell. *Acustica*, 68(2):168–172, 1989.
- [9] J. A. Cosgrove, J. M. Buick, D. M. Campbell, and C. A. Greated. To appear in *Proceedings of the 8th International Congress on Sound and Vibration*, Hong Kong, China, 2001.
- [10] H. Mitome, T. Kozuka, and T. Tuziuti. *Jpn. J. Appl. Phys.*, 34:2584–2589, 1995.
- [11] T. G. Leighton. *The Acoustic Bubble*. Academic Press, 1994.

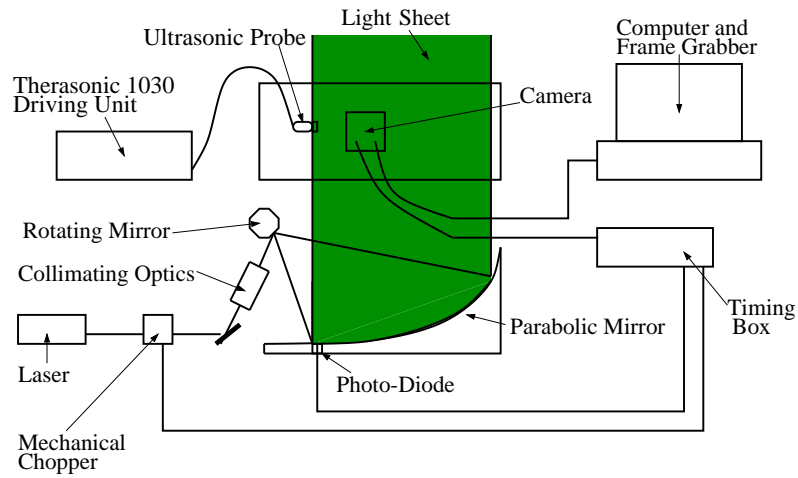


Figure 1: Experimental set-up

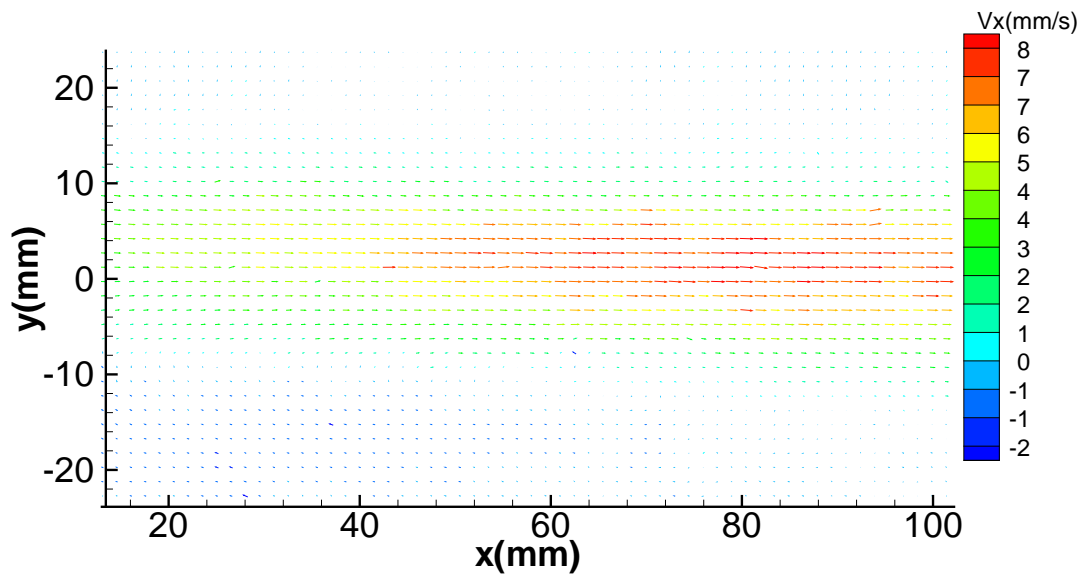


Figure 2: Instantaneous velocity map with probe output set to  $0.25 \text{ Wcm}^{-2}$ . Colours of vectors indicate magnitude of  $v_x$



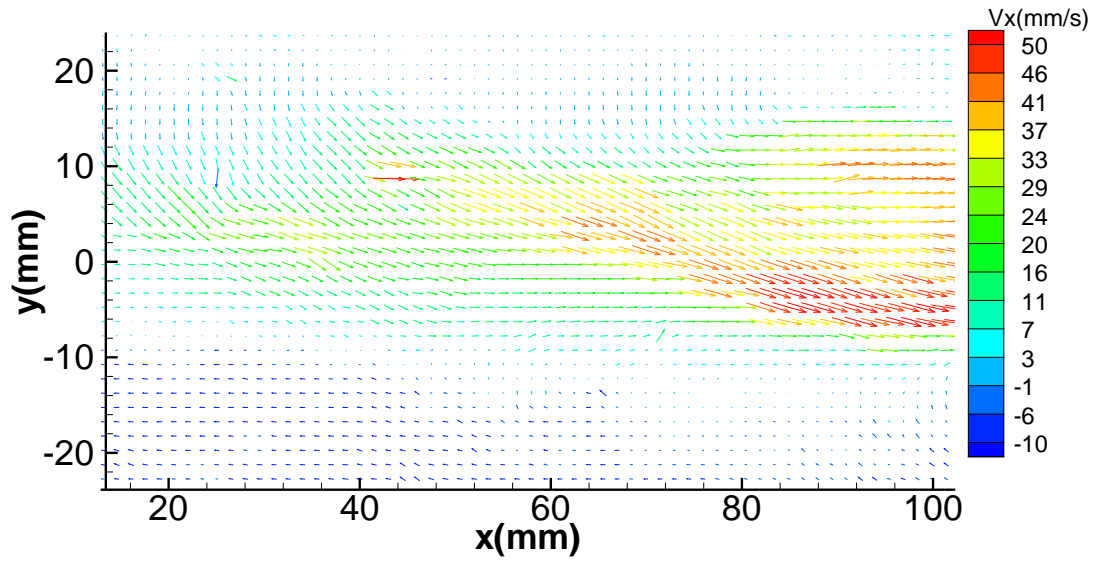


Figure 3: Instantaneous velocity map with probe output set to  $3 \text{ Wcm}^{-2}$ . Colours of vectors indicate magnitude of  $v_x$

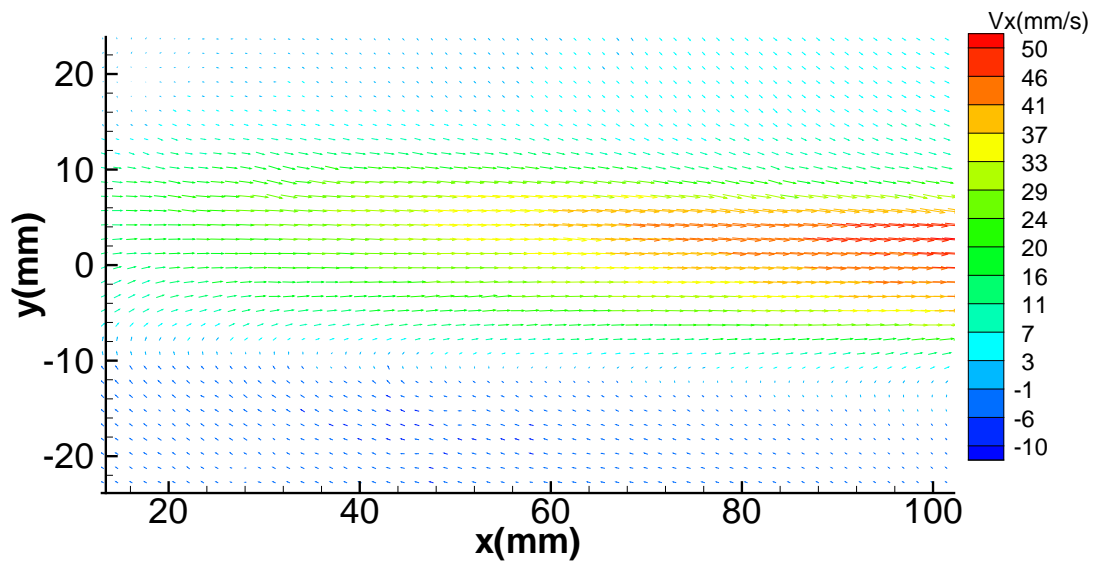


Figure 4: Averaged velocity map with probe output set to  $3 \text{ Wcm}^{-2}$ . Colours of vectors indicate magnitude of  $v_x$

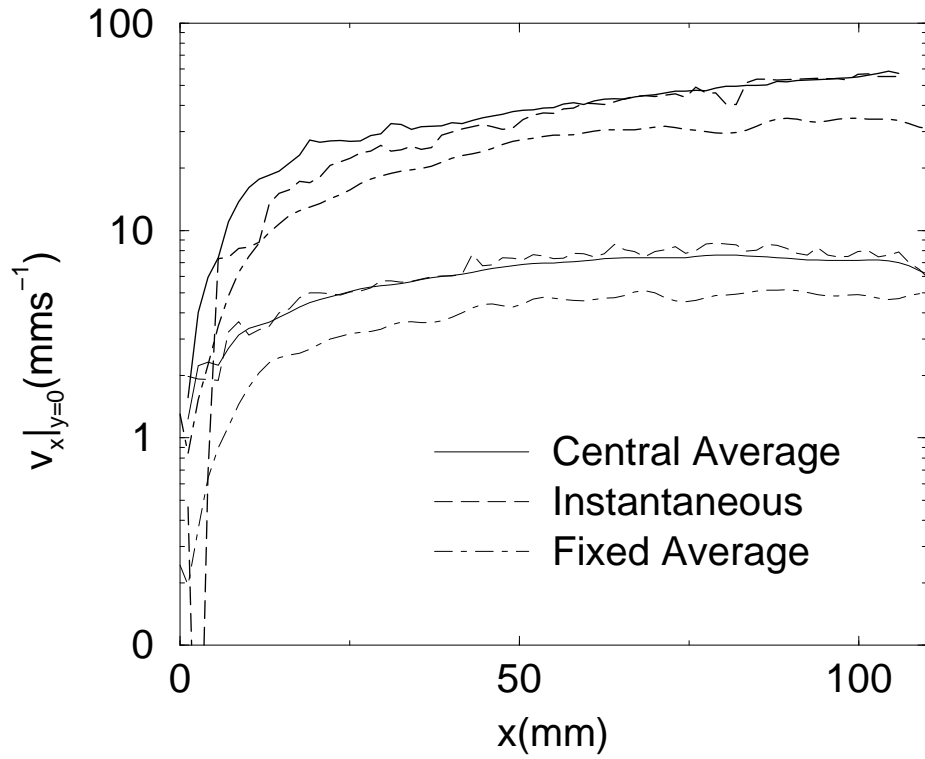


Figure 5: Instantaneous and averaged values of the peak axial velocity. The thick and thin lines are for probe intensities of 3 and  $0.25 \text{ Wcm}^{-2}$  respectively

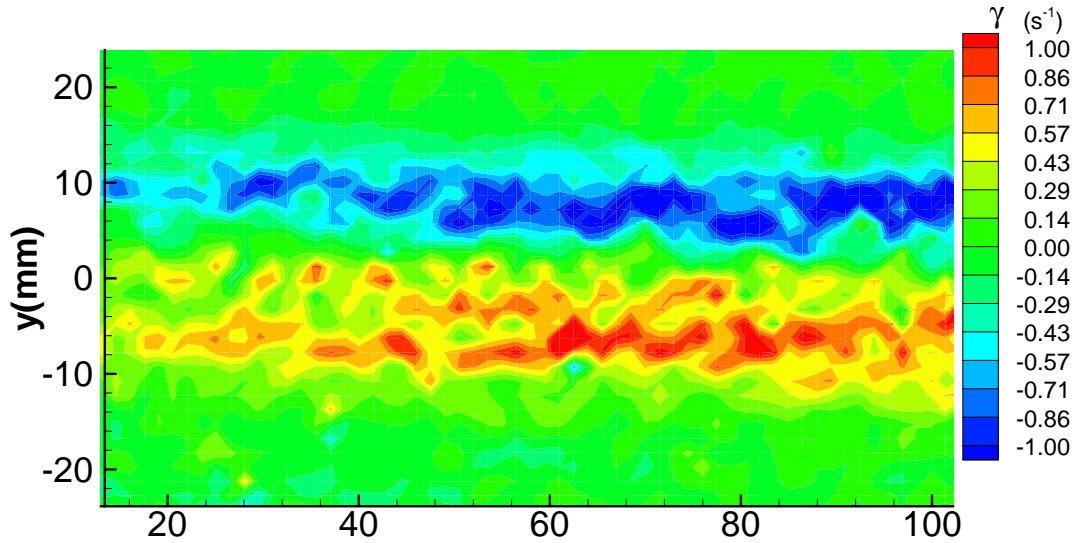


Figure 6: Instantaneous rate-of-shear strain with probe output set to  $0.25 \text{ Wcm}^{-2}$